NIH Public Access
Author Manuscript
Exp Dermatol. Author manuscript; available in PMC 2013 June 01.

Published in final edited form as:
Exp Dermatol. 2012 June ; 21(6): 453–455. doi:10.1111/j.1600-0625.2012.01482.x.

A Direct Method to Determine the Strength of the Dermal – Epidermal Junction in a Mouse Model for Epidermolysis Bullosa

Thomas J. Sproule, **Derry C. Roopenian***, and **John P. Sundberg***
The Jackson Laboratory, Bar Harbor, ME 04609-1500 USA

Abstract

Epidermolysis bullosa (EB) describes a spectrum of rare, incurable, inherited mechanobullous disorders unified by the fact that they are caused by structural defects in the basement membrane zone which disrupt adhesion between the epidermis and dermis. Mouse models provide valuable tools to define the molecular basis of these diseases and to test novel therapeutic approaches. There is need for rapid, quantitative tests that measure the integrity of dermal-epidermal adhesions in such models. To address this need, we describe a novel quantitative method to determine the mechanical strength of the adhesion between tail skin epidermis and dermis. We show that this test reliably measures the force required to cause dermal-epidermal separation in tails of mice that are genetically predisposed to a form of non-Herlitz Junctional EB which develops as the result of a hypomorphic mutation in the laminin gamma 2 gene (*Lamc2*^{jeb}). This simple, quantitative method of directly measuring the tensile strength of dermal-epidermal adhesion provides a novel dimension to the pathophysiological screening, evaluation, and therapeutic treatment of mice that may develop progressive forms of EB and potentially other disorders that compromise cutaneous integrity.

Keywords

junctional epidermolysis bullosa; laminin gamma 2; tail tension test; dermis; epidermis; push-pull force gauge

Introduction

Mammalian skin is a complex organ that carries out multiple biological functions, with its ability to act as a barrier to the outside world being the most critical. To maintain this barrier function, skin must be very flexible, durable, and resistant to force-induced injury (1, 2). The basement membrane is a complex structure that tightly adheres the epidermal and dermal layers in a manner that ensures these mechanical cutaneous properties (3). A group of heritable diseases, known collectively as epidermolysis bullosa (EB), develop as the result of defects in components that weaken this attachment. This weakening ultimately results in dermal – epidermal separation and the characteristic features of EB including skin fragility, blisters, and ulcers. EB can emerge as the result of mutations in a number of known and potentially unknown basement membrane components, and can be highly variable in its subforms and severity (reviewed in (4–7)). Mouse models of human forms of EB provide incisive experimental tools to define cause-effect relationships between molecular defects and pathophysiological consequences (8, 9). However, the analysis of such models has been

Corresponding author: Thomas J. Sproule, The Jackson Laboratory, 600 Main Street, Bar Harbor, ME 04609-1500, Phone: 207-288-6397, Fax: 207-288-6683, tom.sproule@jax.org.
*These authors contributed equally to this work

Conflict of interest: The authors declare no conflicts of interest with respect to the publication of this article.

NIH-PA Author Manuscript
NIH-PA Author Manuscript
NIH-PA Author Manuscript

NIH-PA Author Manuscript

NIH-PA Author Manuscript

NIH-PA Author Manuscript

generally focused on pathological features that are indirectly related to the mechanical defects of the basement membrane. There is a need for quantitative methods that more directly address the overall mechanical integrity of the cutaneous basement membrane. Mice with a hypomorphic mutation in the laminin gamma 2 gene (*Lamc2*^{jeb}) develop a form of non-Herlitz Junctional EB (nH-JEB) with gradual onset (10). Here, we exploit this mouse model to develop a method that directly measures the tensile strength of dermal-epidermal adhesion in adult mouse tail skin.

Materials and Methods

Measurement device design

Major components of the tail tension measurement device, assembled in Figure 1a, include a standard mouse restraining device with a slot to allow the tail to extend beyond (Fig. 1b); a clamp to grip a defined portion of the mouse tail skin including a wire loop for attachment (Fig. 1c, d); a push-pull force gauge capable of measuring 1–100 Newtons (ANF-100 "Success", M.H.M. Co. Ltd, Osaka, Japan) (Fig. 1e); and a cantilevered arm to apply force (Fig. 1a). These components were oriented in a manner to allow the force to pull the clamped tail horizontally directly away from the body. The test stand was manufactured from wood (pine base and hard wood lever assembly), and was sealed with acrylic paint. The restraining device was manufactured from plexiglass (Fig. 1b). The clamp was a ~3 cm^2 brass door hinge lined with two ~2.5 cm^2 squares of gasket rubber that was tightened onto a mouse tail using a stainless steel screw and wing nut (Fig. 1c, d). The gasket rubber was replaced periodically (after ~50–100 mice) to maintain its friction properties. The wire loop was ~4 cm long and made using 20 gauge stainless steel.

Mice

C57BL/6J (B6) wild-type (wt) mice were obtained from JAX Mice & Services (Bar Harbor, ME). B6.129X1-*Lamc2*^{jeb}/Dcr (B6-*Lamc2*^{jeb}) were produced by backcrossing previously described 129X1/SvJ-*Lamc2*^{jeb}/Dcr (10) N11 onto B6 while preserving a 129X1 congenic interval including the *Lamc2*^{jeb} mutation based on genotyping of bracketing dinucleotide repeat spanning markers *D1Dcr2* and *D1Dcr15* (informatics.jax.org), located on mouse chromosome 1 at ~152 and 162 Mb respectively. Male and female B6 wt and B6-*Lamc2*^{jeb}/*Lamc2*^{jeb} homozygotes 4 to 20 weeks of age and male B6-*Lamc2*^{jeb}/*Lamc2*$^{+}$ heterozygotes 20 weeks of age were used. Mice were maintained in a specific pathogen free mouse colony in The Jackson Laboratory's Research Animal Facility under standard husbandry conditions. Animal protocols were reviewed and approved by the Institutional Animal Care and Use Committee.

Measurement procedure

Groups of mice were euthanized by CO_2 asphyxiation and then immediately tested. The distal portion of each tail was excised, leaving ~5 cm of tail attached to the body (Fig. 2a). The tail was then secured in the clamp so that it extended just beyond the gasket rubber squares (Fig. 2b). The mouse was placed in the restraining device, with the tail extending through the slot (Fig. 2c). Care was taken during these steps to avoid unnecessary pulling on the tail, which could cause the skin to separate prematurely or to be damaged. The clamp was then connected to the push-pull force gauge (Fig. 2d), the base of the tail was firmly held between thumb and forefinger (Fig. 2e), and tension was applied by quickly and firmly pulling the cantilever handle (before pulling, Fig. 2f, after pulling, Fig. 2g). Fig. 2h is a close up of the tail after the handle pull, showing that a 'sleeve' of tail skin was removed. Final tension in Newtons was read from the dial of the push-pull force gauge (Fig. 2i).

NIH-PA Author Manuscript

NIH-PA Author Manuscript

NIH-PA Author Manuscript

Histologic evaluation of tail skin sleeves

Representative samples were collected at the completion of the tail sleeve removal, fixed by immersion in Fekete's acid alcohol formalin, processed routinely, embedded in paraffin, sectioned, and stained with hematoxylin and eosin.

Results and Discussion

To evaluate the utility of the tail tension device, we tested the hypothesis that the *Lamc2*^{jeb} mutation resulted in a systemic weakening of tail dermal-epidermal adhesion that would clearly distinguish wt mice from *Lamc2*^{jeb}. Our data supported this hypothesis in two ways. First, in the case of B6 wt and B6-*Lamc2*^{jeb} mice all tension measurements differed substantially when comparing age and sex matched groups ($p < 0.001$ by 2-tailed heteroscedastic t-test, comparing females and males at 11 and 15 weeks of age), with no B6 wt values below 43 N and no B6-*Lamc2*^{jeb} values above 33 N (Fig. 3a, b). Second, this test thoroughly removed the entire tail skin as a 'sleeve' from all B6-*Lamc2*^{jeb} homozygotes but failed to remove any skin from B6 wt-homozygous or *Lamc2*^{jeb}/*Lamc2*$^{+}$ heterozygous mice. Histology confirmed that *Lamc2*^{jeb} skin removal included separation at the dermal-epidermal boundary, as would be expected from a nH-JEB mutation (9) (Fig. 3c-e). All B6 wt homozygote and *Lamc2*^{jeb}/*Lamc2*$^{+}$ heterozygote tests ended in tail breakage or clamp slippage, demonstrating that the force binding epidermis and dermis in wt mice is substantial; exceeding the limits of our testing method and, in cases of tail breakage, the structural limits of ligaments and other connective tissue components of the tail as a unit. Successful shearing of B6-*Lamc2*^{jeb} skin demonstrated that homozygosity of the *Lamc2*^{jeb} mutation weakened the dermal-epidermal mechanical connections sufficiently that it allows quantitative measurements of adhesion in this mouse model.

Of ~550 *Lamc2*^{jeb} homozygote tail tension measurements conducted prior to this writing representing a range of ages and background genetics, 6 (~1%) removed full tail skin 'sleeve' at high tensions (40-44N), 32 (~6%) removed patches of skin at 28-55N and 7 (~1%) involved tail breakage or clamp slippage without skin removal at 28-48N. The remainder (~92%) involved full tail skin removal at <40N. Full tail skin 'sleeve' removal is the most desirable outcome, as it measures the force necessary to cause full dermal-epidermal separation of a specifically sized piece of tail skin (full circumference and 2.5 cm long). The overlap of tail breakage and clamp slippage values with valid 'sleeve' removal values illustrates that they are a form of 'technical failure' which can vary with experimental conditions. For example, thinner tails found on younger mice may be less durable and more subject to breakage, and old rubber clamp liners could have a greater tendency to slip.

In considering whether to accept tension results or decide that they are technical failures, the following guides should apply: 1) All results which include full 'sleeve' removal are valid. Sleeves which are incomplete but remove >50% of the clamped skin are also valid. 2) Tests which remove patches of skin (<50% of clamped area) may be accepted with caution. However, if they tend to occur at lower tensions than 'full sleeve' results, they may indicate that it is time to replace the rubber clamp inserts. 3) Tension tests which do not remove obvious patches of skin should only be accepted if reproducible under best conditions (good tail support and new rubber clamp inserts).

The pathophysiological features of EB result from structural defects which weaken dermal-epidermal adhesion. This study describes a rapid quantitative method to directly evaluate this mechanical property in mouse models for these diseases. We demonstrate the phenomenon of skin separation due to minor shear forces in a mouse model of nH-JEB that develops a progressive disease because of the hypomorphic *Lamc2*^{jeb} mutation. The force values in mice genetically sensitized for structural weakness because of the *Lamc2*^{jeb}

NIH-PA Author Manuscript

NIH-PA Author Manuscript

NIH-PA Author Manuscript

mutation result in highly reproducible results among mice of the same age and sex. Typically tail skin lesions and ear lesions only become observable after 12 weeks of age in B6-*Lamc2*^{jeb} homozygotes (results not shown). Reduced tensile strength is observed in *Lamc2*^{jeb} homozygotes as early as measurements are practical (4 weeks of age) and well before such lesions are apparent. While the results clearly show a systemic dermal – epidermal weakness observable in both sexes, this weakness also increases over time. Comparisons of sequential time points show significant decreases in adhesion in B6-*Lamc2*^{jeb} homozygote females between 15 and 19 weeks and in B6-*Lamc2*^{jeb} homozygote males between 6 and 11 weeks, and again between 11 and 15 weeks. This progressive weakening is more apparent in B6-*Lamc2*^{jeb} males (Fig. 3a, b), which develop gross lesions at an earlier age compared with females (Sproule, *et al.*, manuscript in preparation). Taken together, the results from the tension test assay therefore demonstrate a generalized cutaneous structural weakness as the result of the *Lamc2*^{jeb} allele that progresses, ultimately resulting in the prototypic pathological features of nH-JEB.

This method is well-suited for models of EB in which the disease develops in adult mice, but is not obviously applicable to models of severe Herlitz forms of EB that result in perinatal lethality or failure of the mouse to survive into adulthood, such as *Lamc2*^{tm1Uit}. It provides a simple method for the assessment of the effects of background genetic modifiers on mouse models of adult-onset structural blistering diseases including but potentially not limited to nH-JEB, and the response of such mice to therapies. The method additionally provides a novel assay to identify alleles that result in cutaneous weakness in forward genetic mutagenesis screens and in reverse genetic phenotypic assessment of genetically-engineered mice as part of the Knockout Mouse Project (www.komp.org).

Acknowledgments

This work was supported by grants from the National Institutes of Health (AR054407) and the DeBRA Foundation. TJS conceived and developed the assay and conducted the research. All authors contributed significantly to the design of the study, interpretation and preparation of the manuscript. We thank V. Sun for assistance with photography and J. Hammer for his assistance with figure preparation.

Abbreviations

EB	epidermolysis bullosa
nH-JEB	non-Herlitz Junctional Epidermolysis Bullosa
Lamc2	laminin gamma 2 gene symbol
B6	C57BL/6J
B6-*Lamc2*^{jeb}	B6.129X1-*Lamc2*^{jeb}/Dcr
wt	wild-type
N	Newtons

References

1. Chuong CM, Nickoloff BJ, Elias PM, et al. What is the 'true' function of skin? Exp Dermatol. 2002; 11:159–187. [PubMed: 11994143]
2. Sundberg, JP.; Nanney, LB.; Fleckman, P.; King, LE. Skin and adnexa. In: Treuting, PDS.; Frevert, CW.; Liggitt, D.; Montine, KS., editors. Comparative anatomy and histology A mouse and human atlas. Amsterdam: Academic Press; 2012. p. 433-455.
3. Aumailley M, Smyth N. The role of laminins in basement membrane function. J Anat. 1998; 193 (Pt 1):1–21. [PubMed: 9758133]

NIH-PA Author Manuscript

NIH-PA Author Manuscript

NIH-PA Author Manuscript

4. Fine JD, Eady RA, Bauer EA, et al. The classification of inherited epidermolysis bullosa (EB): Report of the Third International Consensus Meeting on Diagnosis and Classification of EB. J Am Acad Dermatol. 2008; 58:931–950. [PubMed: 18374450]

5. Uitto J, McGrath JA, Rodeck U, Bruckner-Tuderman L, Robinson EC. Progress in epidermolysis bullosa research: toward treatment and cure. J Invest Dermatol. 2010; 130:1778–1784. [PubMed: 20393479]

6. Bruckner-Tuderman L, McGrath JA, Robinson EC, Uitto J. Animal models of epidermolysis bullosa: update 2010. J Invest Dermatol. 2010; 130:1485–1488. [PubMed: 20463671]

7. Natsuga K, Shinkuma S, Nishie W, Shimizu H. Animal m;odels of epidermolysis bullosa. Dermatol Clin. 2009; 28:137–142. [PubMed: 19945627]

8. Jiang QJ, Uitto J. Animal models of epidermolysis bullosa--targets for gene therapy. J Invest Dermatol. 2005; 124:xi–xiii. [PubMed: 15812910]

9. Varki R, Sadowski S, Pfendner E, Uitto J. Epidermolysis bullosa. I. Molecular genetics of the junctional and hemidesmosomal variants. J Med Genet. 2006; 43:641–652. [PubMed: 16473856]

10. Bubier JA, Sproule TJ, Alley LM, et al. A mouse model of generalized non-Herlitz junctional epidermolysis bullosa. J Invest Dermatol. 2010; 130:1819–1828. [PubMed: 20336083]

NIH-PA Author Manuscript
NIH-PA Author Manuscript
NIH-PA Author Manuscript

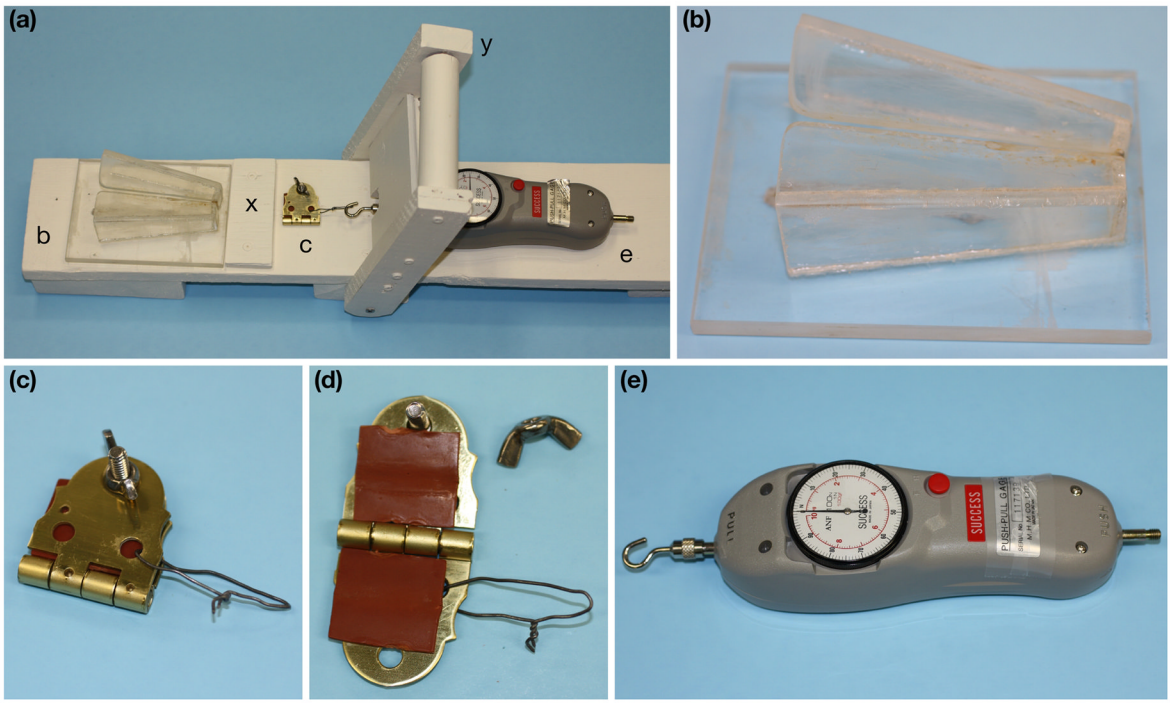

Figure 1.
Test stand with components left to right: Complete test assembly (a), plexiglass restraining device (b), clamp (c) with gasket rubber (d), wire loop (c, d), and the hook and push-pull force gauge (e). Also labeled are the restraining device stop board (x) and the cantilever handle (y) which is pulled (left to right) to conduct the test.

NIH-PA Author Manuscript
NIH-PA Author Manuscript
NIH-PA Author Manuscript

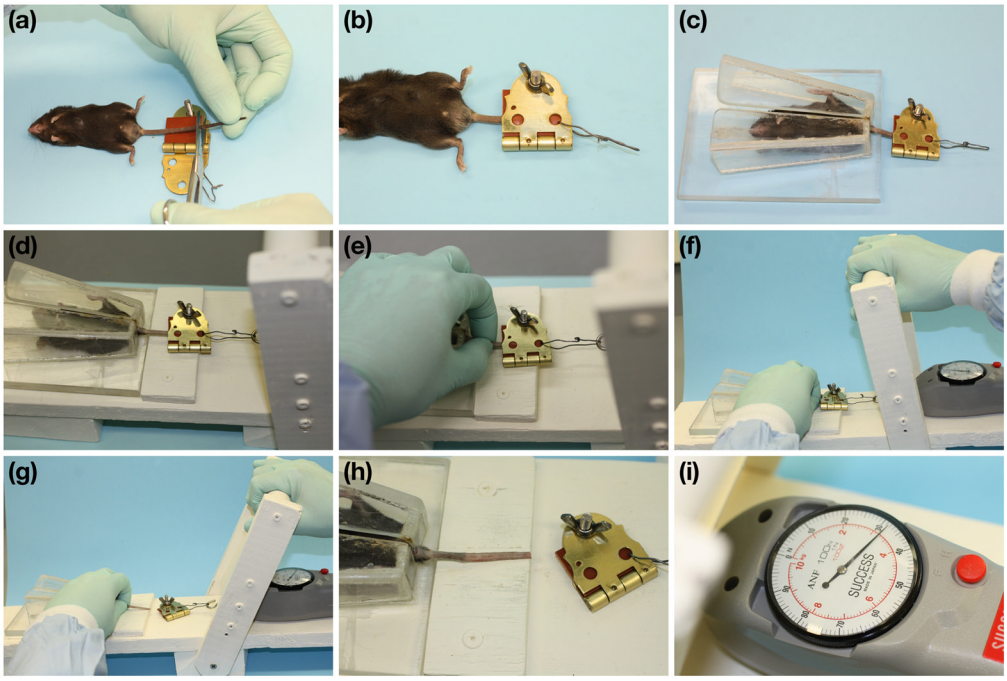

Figure 2.
Step-by-step tail tension procedure: Tail of euthanized mouse is cut so ~5 cm remain (a). Tail is clamped (b). Mouse is placed in restraining device with tail through opening so clamp is outside (c). Clamp is attached to force gauge on test stand (d). Tail is supported with thumb and forefinger (e). Cantilever handle is pulled away from tail (f, before; g, after). Tail shown after clamp pulled away, with skin 'sleeve' removed (h). Tension to remove skin sleeve is read from force gauge (i).

NIH-PA Author Manuscript

NIH-PA Author Manuscript

NIH-PA Author Manuscript

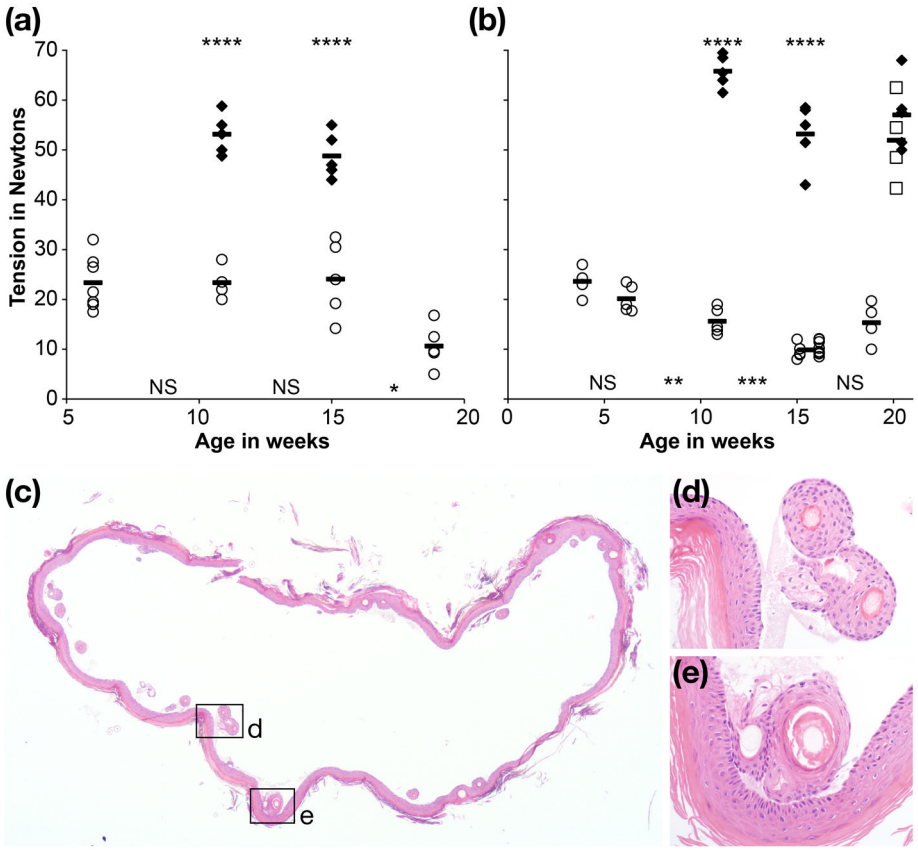

Figure 3.

Tension results for female (a) and male (b) B6 wt (filled diamond), B6-*Lamc2*^{jeb} homozygotes (open circle) and B6-*Lamc2*^{jeb}/*Lamc2*$^{+}$ heterozygotes (open squares) at the ages indicated (n = 4–14 per group). All B6 wt and B6-*Lamc2*^{jeb}/*Lamc2*$^{+}$ heterozygote tension values measured the force at which tissue failed or clamp slipped off without removing the tail skin. All B6-*Lamc2*^{jeb} homozygote measurements shown include successful removal of tail skin 'sleeve'. In all cases age matched B6 wt and B6-*Lamc2*^{jeb} homozygote values were highly significantly different ($p < .001$ for both females and males at 11 and 15 weeks (****)). In compared sequential sets of B6-*Lamc2*^{jeb} homozygotes, females at 15 vs 19 weeks ($p = .013$ (*)) and males at 6 vs 11 weeks ($p = .027$ (**)) and 11 vs 15 weeks of age ($p = .006$ (***)) significantly differed. All other adjacent age sets had $p > .05$ (NS). B6-*Lamc2*^{jeb}/*Lamc2*$^{+}$ heterozygote values at 20 weeks did not significantly differ from B6 wt at 20 weeks ($p = .38$) but did significantly differ from B6-*Lamc2*^{jeb} homozygotes at 19 weeks ($p = .001$). The statistical evaluations use the 2-tailed heteroscedastic t-test. Histology of a cross-section of a representative tail skin sleeve from a *Lamc2*^{jeb} homozygote (c). Enlarged boxed areas (d, e) reveal complete dermal-epidermal separation without dermal adhesion or loss of the contiguous hair follicles confirming that the test is indeed measuring dermal-epidermal separation due to weak basement membranes that are defective in this mouse model. H&E.